Helical strain in carbon nanotubes: Speed of sound and Poisson ratio from first principles

H. M. Lawler,[1] J. W. Mintmire,[2] and C. T. White[1]
[1]*Chemistry Division, Naval Research Laboratory, Washington, DC 20375, USA*
[2]*Department of Physics, Oklahoma State University, Stillwater, Oklahoma 74078, USA*
(Received 26 May 2006; revised manuscript received 3 August 2006; published 15 September 2006)

We detail a formalism describing the elastic response from helical strains and demonstrate that it is a natural application of a first-principles method which treats the electronic structure with helical symmetry. We then derive a helical strain matrix, giving analytic expressions for Poisson's ratio and the longitudinal and torsional speeds of sound, which are calculated from first principles for a large set of nanotube structures. The results indicate that the speed of sound and Poisson's ratio are to good approximation independent of nanotube structure and can be ascertained by consideration of the elastic response in bulk graphite.

DOI: 10.1103/PhysRevB.74.125415 PACS number(s): 62.20.Dc, 62.25.+g, 62.30.+d

In the low-temperature regime, velocities of sound are key quantities for transport properties in solid-state systems. Indirectly, they limit the ballistic conduction and govern the temperature dependence of the nonballistic behavior through their determination of the thermal occupation of the scattering phonons. More directly, they give the heat flux carried by acoustic modes. For these reasons, precise knowledge of the speeds of sound is important to detailed analysis of performance in many low-temperature applications of nanotechnology, such as thermoelectric conversion, thermal dissipation, and the temperature dependence of electrical conduction.[1]

Despite their fundamental significance and unequivocal physical interpretation, the extensive literature on nanotube elasticity typically emphasizes various strain coefficients and elastic moduli over the sound velocities. This might be partly because of the authors' interest in properties relating to mechanical rigidity and load response,[2] and partly because the sound velocities are regarded as a derivative quantity easily obtained from the more general strain characteristics. Nevertheless, the theoretical nanotube elastic moduli are usually reported in units of pressure,[3,4] which is a bulk quantity. For the conversion to sound velocity, a mass density by volume is required, a quantity not entirely natural in a lower dimensional structure such as a nanotube, requiring either a "wall thickness" or an energy density unphysically bounded by the nanotube wall for interpretation. In several published studies, applications of the "thin-shell" model have consistently calculated non-negligible structure dependence of elastic moduli and Poisson ratios,[5] particularly for nanotubes of diameter less than 1 nm. However, a tight-binding calculation of the speeds of sound, extrapolated from the phonon dispersions, reported negligible diameter dependence of the sound velocities and a very weak chiral dependence.[6]

For the sake of quantitative understanding of the speed of sound in nanotubes and its structure dependence, we have formulated a quasi-one-dimensional strain theory specific to helical systems. As a helical formalism, the elastic theory we describe is a natural application of a density-functional method which solves for the electronic ground state subject to the screw-symmetric boundary conditions.[7] By combining the strain analysis with this method, we have performed calculations for nearly every nanotube structure within the 0.40–1.40 nm diameter range. We shall demonstrate that the symmetric, nine-element strain matrix conveys the radial-breathing mode diameter dependence, Poisson's ratio, and both torsional and longitudinal speeds of sound.

The elastic coefficients we introduce relate the total energy per atom to dimensionless, helical-symmetry specific strain amplitudes. Through a system of second-order partial derivatives of the energy with respect to the strains, a helical Bloch-phase dependent strain matrix is derived, which conveys a range of elastic information, such as the quantities mentioned above. (The transverse flexural modes[8] cannot be addressed with the formalism at hand, because the atomic displacements involved are not invariant with application of the screw operation.)

As helical polymers, nanotubes exhibit invariance with respect to successive application of a screw operation, $\hat{\mathbf{S}}(\varphi_0, h_0)$, and it can be considered as a Bloch operation. The parameters φ_0 and h_0 are rotation and translation, respectively, and are expressed in terms of the rolling vector of the nanotube (m_1, m_2), written in the basis of the triangular Bravais lattice vectors.[9]

By first considering a reference cell whose position, in cylindrical coordinates, is $\mathbf{P}=(R_0,0,0)$—where the first component is the distance from the nanotube axis, the second component is the azimuthal angle, and the third component is the distance along the axis—a nanotube of infinite one-dimensional extent can then be generated by repeated application of the screw operation. The reference cell at the point $\mathbf{P}$ contains $2N$ basis carbon atoms for a nanotube with an N-fold rotational symmetry about its axis. The coordinates of the nth cell, then, are

$$\mathbf{n}_0 = \hat{\mathbf{S}}^n \mathbf{P} = (R_0, n\varphi_0, nh_0). \tag{1}$$

We are concerned with generalized strain fields of the cell positions, given by Eq. (1), which are now rewritten as

$$\mathbf{n}_0 = (R_0, n\varphi_0, nh_0) = (R_n, \varphi_n, h_n). \tag{2}$$

Formally, the independence of the radial coordinate from n is related to the fact that the screw symmetry requires that the radial displacement field be even with respect to n, while the longitudinal and torsional strain fields must be odd. More physically, these statements imply that there is no acoustic condition on radial displacements; that is, that there are no

zero-frequency radial modes. Nevertheless, we will retain the radial displacement field in our consideration of the helical elasticity theory, because it allows for the derivation of familiar quantities, such as Poisson's ratio.

Now let us consider the three helical strains,

$$R_n \to (1+\varepsilon_R)R_n = (1+\varepsilon_R)R_0,$$

$$\varphi_n \to (1+\varepsilon_\varphi)\varphi_n = (1+\varepsilon_\varphi)n\varphi_0,$$

and

$$h_n \to (1+\varepsilon_h)h_n = (1+\varepsilon_h)nh_0, \tag{3}$$

so that

$$\mathbf{n}_0 \to \mathbf{n}_0 + \boldsymbol{\delta n}, \tag{4}$$

with

$$\boldsymbol{\delta n} = (\varepsilon_R R_0, n\varepsilon_\varphi \varphi_0, n\varepsilon_h h_0). \tag{5}$$

While additional strains which mix the coordinates can occur (such as flexural strains), such configurations violate the screw symmetry and will not be considered here.

We would now like to express $\boldsymbol{\delta n}$ as a sinusoidal displacement field. With this ansatz, we can relate the right side of Eq. (3) to the periodic displacement amplitudes,

$$(1+\varepsilon_R)R_0 = R_0 + A_R \cos[\kappa n],$$

$$(1+\varepsilon_\varphi)n\varphi_0 = n\varphi_0 + A_\varphi \sin[\kappa n], \tag{6}$$

and

$$(1+\varepsilon_h)nh_0 = nh_0 + A_h \sin[\kappa n],$$

with κ equal to the Bloch phase obtained per application of the screw operation. The elastic strain condition implies a slow phase variation, so that $\kappa \ll 1$. With respect to the integer site index, n, the above choices of even and odd displacement fields ensure that Eq. (6) is consistent to lowest order in n. Rewriting Eq. (5) according to the above gives

$$\boldsymbol{\delta n} = (A_R \cos[\kappa n], A_\varphi \sin[\kappa n], A_h \sin[\kappa n]). \tag{7}$$

Subtracting the equilibrium positions from both sides in Eq. (6), we then can immediately write expressions for the strain parameters of Eq. (5) in terms of the wave-form parameters from Eq. (7). With Eq. (7) expanded to lowest order in n, the expressions give

$$\varepsilon_R = \frac{A_R}{R_0}, \quad \varepsilon_\varphi = \kappa\frac{A_\varphi}{\varphi_0}, \quad \varepsilon_h = \kappa\frac{A_h}{h_0}. \tag{8}$$

Finally, we note, that the displacement field in Eq. (3) can be modeled through corresponding changes in the generating screw operation and nanotube radius,

$$\hat{\mathbf{S}}(\varphi_0, h_0) \to \hat{\mathbf{S}}(\varphi_0 + \delta\varphi_0, h_0 + \delta h_0), \quad R_0 \to R_0 + \delta R_0. \tag{9}$$

The condition which makes the strain field of Eq. (9) consistent with Eq. (3) is

$$\varepsilon_R = \frac{\delta R_0}{R_0}, \quad \varepsilon_\varphi = \frac{\delta\varphi_0}{\varphi_0}, \quad \varepsilon_h = \frac{\delta h_0}{h_0}. \tag{10}$$

Through comparison of Eqs. (8) and (10), we have at this point accomplished simple formulas relating helical longwave behavior with perturbations of the generating screw operation. These relations are analogous to elasticity theory in bulk crystals, where the effect of strain perturbation on longwave parameters is related to its effect on the parameters entering the generating translation vectors.[10]

Because our first-principles method is fundamentally helical, the strain calculations of Eq. (10) require no special consideration. We have performed extensive calculations of this type, and we shall see that the results imply that to first approximation, the two speeds of sound in nanotubes and the Poisson's ratio are independent of structure and can be inferred from the elastic properties of graphite.

So far we have demonstrated a helical strain theory and its connection to longwave displacements and pointed out that a helical electronic structure method is immediately suited for its numerical evaluation. To obtain speeds of sound, the elastic energetics must be introduced. We can write the elastic strain energy in the standard quadratic way,

$$U = \tfrac{1}{2}\Sigma_{ij} c_{ij}\varepsilon_i\varepsilon_j, \tag{11}$$

where the c_{ij} is the "force constant" associated with the strain amplitudes of Eqs. (3), (8), and (10). An important point is that these elastic constants are in units *energy* rather than *energy density*, which allows for derivations of sound velocities without introducing somewhat artificial length parameters.

With the specialized density-functional method mentioned above,[7] evaluation of the elastic constants for a large set of nanotube diameters and chiralities, c_{ij}, is a straightforward procedure. The strain states are modeled within the adiabatic approximation so that a self-consistent electronic ground state is obtained for each strain configuration. Evaluations of the elastic constants, c_{ij}, are then accomplished with simple polynomial fits to the ground-state energy's dependence on the strain amplitudes. The linear-combination-of-atomic-orbital, Gaussian basis set for the all-electron density-functional calculations included $7s3p$ functions, and the Kohn-Sham orbitals were sampled for 36 values of the helical Bloch phase over the one-dimensional Brillouin zone.

The initial structural information is adopted from rolled graphene, an approximation which, in earlier work, proved sufficient for lattice dynamical calculations even to the smallest-diameter nanotubes reported here.[11] The frozen-phonon strain amplitudes were selected so that $\varepsilon_R R_0$, $\varepsilon_\varphi R_0\varphi_0$, and $\varepsilon_h h_0$ varied within the range of 3×10^{-4} to 2×10^{-3} nm. In the evaluation of c_{hh} and $c_{\varphi\varphi}$, the energetic response was calculated at six values of strain about the initial geometry. For these quantities, cubic and quartic contributions to the stresss fields were subtracted before establishing the quadratic contribution of interest. In the evaluation of c_{Rh}, five radial strains were introduced for each of two, positive and negative, longitudinal strains. Through a quadratic fit, the linear contribution of the radial strain to the potential energy was obtained for each longitudinal strain, and the two values were subtracted for the appropriate second derivative. Checks were performed to verify that switching longitudinal

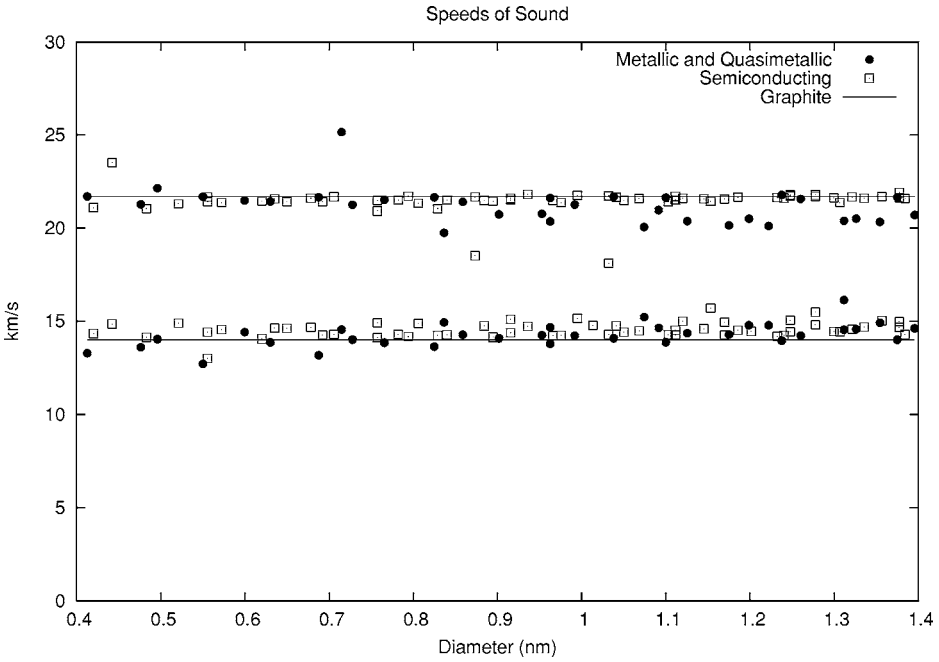

FIG. 1. The calculated longitudinal and torsional speeds of sound in 93 nanotubes for the diameter range shown. The horizontal lines are the measured speeds in graphite, as referenced in the text.

and radial strain amplitudes in the numeric procedure did not significantly affect the results.

In our strain calculations, the distortions strain the reference cell as well as the screw parameters. So if the equilibrium relative coordinates between two atoms interior to the reference cell are (τ_φ, τ_h), then after the strain they are $\tau_\varphi \rightarrow (1+\tau_h \varepsilon_\varphi / h_0)\tau_\varphi$ and $\tau_h \rightarrow (1+\varepsilon_h)\tau_h$. These cell strains conserve the longitudinal and rotational strains per unit length along the nanotube.

Substituting Eq. (8) into Eq. (11), we can write the elastic energy in terms of the wave-form parameters,

$$U = \frac{1}{2} c_{RR} \left(\frac{A_R}{R_0} \right)^2 + \frac{1}{2} \kappa^2 \left[c_{\varphi\varphi} \left(\frac{A_\varphi}{\varphi_0} \right)^2 + c_{hh} \left(\frac{A_h}{h_0} \right)^2 + 2 c_{\varphi h} \left(\frac{A_\varphi}{\varphi_0} \frac{A_h}{h_0} \right) \right] + \kappa \left[c_{R\varphi} \left(\frac{A_\varphi}{\varphi_0} \frac{A_R}{R_0} \right) + c_{Rh} \left(\frac{A_h}{h_0} \frac{A_R}{R_0} \right) \right]. \tag{12}$$

We are now ready to write the strain matrix. It is the force-constant matrix associated with Eq. (12),[12]

$$D_{ij} = -\frac{1}{M} \frac{\partial^2 U}{\partial A_i \partial A_j}. \tag{13}$$

In Eq. (13), the azimuthal amplitude is implicitly scaled by the nanotube radius, and the carbon nuclear mass is indicated by M. From Eq. (12), let us write the strain matrix explicitly

$$\mathbf{D} = \begin{pmatrix} -\frac{c_{RR}}{MR_0^2} & -\kappa \frac{c_{R\varphi}}{MR_0^2 \varphi_0} & -\kappa \frac{c_{Rh}}{MR_0 h_0} \\ -\kappa \frac{c_{R\varphi}}{MR^2 \varphi_0} & -\kappa^2 \frac{c_{\varphi\varphi}}{MR_0^2 \varphi_0^2} & -\kappa^2 \frac{c_{\varphi h}}{MR_0 \varphi_0 h_0} \\ -\kappa \frac{c_{Rh}}{MR_0 h_0} & -\kappa^2 \frac{c_{\varphi h}}{MR_0 \varphi_0 h_0} & -\kappa^2 \frac{c_{hh}}{Mh_0^2} \end{pmatrix}. \tag{14}$$

The speeds of sound are derived by first solving for the acoustic phonon frequencies with the eigenrelation

$$|D_{ij} - \omega^2 \delta_{ij}| = 0, \tag{15}$$

and then scaling the helical group velocity with the translation length

$$\mathbf{v}_\lambda = h_0 \frac{\partial \omega_\lambda}{\partial \kappa}. \tag{16}$$

For the purposes of deriving the speeds of sound, we neglect the off-diagonal terms in the strain matrix of Eq. (14). (The nonzero Poisson's ratio which we calculate, for instance, does violate this diagonal approximation but affects the longitudinal speed of sound by just a few percent.) With Eqs. (14)–(16) the torsional speed of sound is

$$\mathbf{v}_\varphi = \frac{h_0}{R_0 \varphi_0} \sqrt{\frac{c_{\varphi\varphi}}{M}}, \tag{17}$$

and similarly, the longitudinal speed of sound is

$$\mathbf{v}_h = \sqrt{\frac{c_{hh}}{M}}. \tag{18}$$

Figure 1 represents the velocities we calculate for the 93 nanotube structures within the diameter range 0.40–1.40 nm, omitting the (15,0), (16,0), and (17,0) nanotubes. (Our code does not take advantage of the pure rotational symmetry of the nanotubes, and so for a given diameter, the zigzag nanotubes require much more computation time than the other structures. For this reason the largest zigzag nanotubes are omitted.) The velocities are approximately constant, 21 km/s for the longitudinal mode and 14 km/s for the torsional mode. The uncertainty in the calculated velocities is 10%, and the anomalous points in the plot—near diameters of 0.72, 0.87, and 1.03 nm—are the longitudinal speed of sound for the (9,0) nanotube and the torsional speeds of sound for

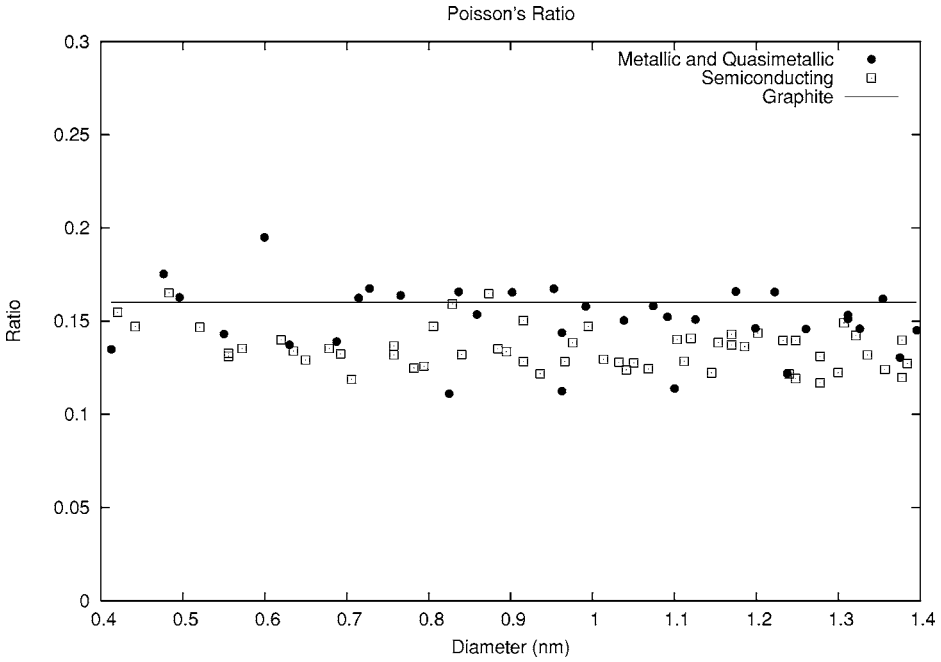

FIG. 2. The calculated Poisson ratios for 91 nanotubes within the diameter range shown and the measured value in graphite.

the (11,0) and (13,0) nanotubes, respectively. We cannot explain these enhancements and assume them to be spurious.

From Fig. 1 it can be seen that the mean values we calculate agree to within precision with the measured in-plane sound velocities in graphite,[13] indicated in the figure with the horizontal lines. There is also agreement with the values obtained from cylindrical continuum theory.[14] The figure depicts a negligible diameter dependence in the speeds of sound we calculate. The chirality dependence is also negligible. For instance, the sound velocities for the nine zigzag and eight armchair nanotubes for which calculations were performed do not differ, excluding consideration of the three anomalous values. The average torsional and longitudinal speeds of sound for the armchair nanotubes are 13.6 and 21.7 km/s, and for the zigzag tubes 14.0 and 21.5 km/s. This insensitivity to the nanotube chiral angle is reflected throughout the other calculations as well.

Semiconducting nanotubes are indicated distinctly from metallic and quasimetallic structures in the figure. No meaningful distinction could be made in the properties of the specimen types, consistent with the results stated above for the armchair nanotubes, which are metallic. In a previous study,[11] we found a slow convergence of the radial strain response for the quasimetallic nanotubes. No similar effect was found for the strain properties reported here, suggesting that the longitudinal and torsional response are less sensitive to relaxation at the Fermi level.

The similarity between the appropriate elastic quantities in graphite and in nanotubes, and among the various nanotube structures, is consistent with other recent calculations[15] and suggests that the correspondence in the speeds of sound is a consequence of universal elastic properties in graphitic systems. It implies that the speeds of sound are primarily surface phenomena, independent of nanotube curvature and chirality to a first approximation. These conclusions indicate that the longwave behavior in nanotubes can be immediately inferred from established elastic properties of bulk graphite. Any calculated nanotube phonon dispersion can therefore be evaluated for the correct acoustic behavior.

As a further application of the helical strain theory, the Poisson's ratio of nanotubes and its relation to that of graphite are now investigated. The Poisson's ratio is a convenient quantity in terms of the strain parameters introduced, as can be seen by imposing a longitudinal strain, and requiring the radial equilibrium condition on Eq. (11),

$$\frac{\partial U}{\partial \varepsilon_R} = 0. \tag{19}$$

The equilibrium ratio of the strains is then

$$\frac{\varepsilon_R}{\varepsilon_h} = \frac{c_{Rh}}{c_{RR}}, \tag{20}$$

which is the Poisson's ratio.

Recently[11] we performed extensive calculations and analysis of the radial-breathing mode and its dependence on nanotube diameter. Through elementary analysis of the harmonic behavior, the radial-mode frequency's inverse diameter dependence can be expressed with the relation

$$\omega_R = \frac{1}{R_0}\sqrt{\frac{c_{RR}}{M}}, \tag{21}$$

which is most conveniently evaluated in atomic units. Our calculations establish that as expected, c_{RR} is independent of nanotube structure to an excellent approximation and takes the value 2.1 Hartree. Within this approximation, for the Poisson's ratio then, our calculations of c_{Rh} are sufficient, according to Eq. (20).

In Fig. 2, we plot the results of these calculations and the measured Poisson's ratio in graphite.[16] The uncertainty in our calculated ratios is taken to be 15% and the (13,0), (14,0), (15,0), (16,0), and (17,0) nanotubes are omitted. The results are similar to another first-principles study of the Poisson ratio for a set of achiral nanotubes.[17]

While several studies have proposed non-negligible diameter dependence in the Poisson ratio, particularly for nanotubes of diameter less than 1 nm, our calculations show no discernible structure dependence with the diameter range 0.40–1.40 nm. These results indicate that, like the speeds of sound and radial elastic coefficient c_{RR}, the Poisson ratio and off-diagonal coefficient c_{Rh} derive from the underlying graphitic nature of the nanotubes.

In summary, we derive a helical elasticity theory to complement a unique first-principles method toward calculating the elastic properties of carbon nanotubes and their variation with structure. The helical theory provides convenient descriptions for a range of elastic behavior, including the radial-breathing mode, longitudinal and torsional speeds of sound, and the Poisson's ratio. The accompanying calculations for more than 90 different nanotube structures indicate that all the quantities considered correspond to those of graphite and exhibit no meaningful structural dependence.

ACKNOWLEDGMENTS

H.M.L. thanks the National Research Council (NRC) for support through a NRC-NRL Resident Research Associateship. This work was also supported by the Office of Naval Research both directly and through the Naval Research Laboratory.

[1] J. Hone, I. Ellwood, M. Muno, A. Mizel, M. L. Cohen, A. Zettl, A. G. Rinzler, and R. E. Smalley, Phys. Rev. Lett. **80**, 1042 (1998); S. Berber, Y-K. Kwon, and D. Tomańek, *ibid.* **84**, 4613 (2000); G. Pennington and N. Goldsman, Phys. Rev. B **68**, 045426 (2003).

[2] E. W. Wong, P. E. Sheehan, and C. M. Lieber, Science **277**, 1971 (1997); B. I. Yakobson, C. J. Brabec, and J. Bernholc, Phys. Rev. Lett. **76**, 2511 (1996).

[3] V. N. Popov, V. E. Van Doren, and M. Balkanski, Phys. Rev. B **61**, 3078 (2000).

[4] J. P. Lu, Phys. Rev. Lett. **79**, 1297 (1997); J. B. Wang, X. Guo, H. W. Zhang, L. Wang, and J. B. Liao, Phys. Rev. B **73**, 115428 (2006).

[5] L. Wang, Q. Zheng, J. Z. Liu, and Q. Jiang, Phys. Rev. Lett. **95**, 105501 (2005); L. Shen and J. Li, Phys. Rev. B **69**, 045414 (2004); S. Gupta, K. Dharamvir, and V. K. Jindal, Phys. Rev. B **72**, 165428 (2005).

[6] J. Yu, R. K. Kalia, and P. Vashishta, J. Chem. Phys. **103**, 6697 (1995).

[7] J. W. Mintmire, in *Density Functional Methods in Chemistry*, edited by J. K. Labanowski and J. W. Andzelm (Springer-Verlag, New York, 1991), pp. 125–137; J. W. Mintmire, B. I. Dunlap, and C. T. White, Phys. Rev. Lett. **68**, 631 (1992); J. W. Mintmire and C. T. White, *ibid.* **50**, 101 (1983).

[8] G. D. Mahan and G. S. Jeon, Phys. Rev. B **70**, 075405 (2004).

[9] C. T. White and J. W. Mintmire, J. Phys. Chem. B **109**, 52 (2005); C. T. White, D. H. Robertson, and J. W. Mintmire, Phys. Rev. B **47**, 5485 (1993).

[10] C. Kittel, *Introduction to Solid State Physics*, 3rd ed. (Wiley, New York, 1966).

[11] H. M. Lawler, D. Areshkin, J. W. Mintmire, and C. T. White, Phys. Rev. B **72**, 233403 (2005).

[12] H. M. Lawler, E. K. Chang, and E. L. Shirley, Phys. Rev. B **69**, 174104 (2004).

[13] R. Nicklow, N. Wakabayashi, and H. G. Smith, Phys. Rev. B **5**, 4951 (1972).

[14] G. D. Mahan, Phys. Rev. B **65**, 235402 (2002).

[15] J. T. Alford, B. A. Landis, and J. W. Mintmire, Int. J. Quantum Chem. **105**, 767 (2005).

[16] O. L. Blakslee, D. G. Proctor, E. J. Seldin, G. B. Spence, and T. Wang, J. Appl. Phys. **41**, 3373 (1970).

[17] D. Sánchez-Portal, E. Artacho, J. M. Soler, A. Rubio, and P. Ordejón, Phys. Rev. B **59**, 12678 (1999).